

ON THE TARGET CLASSIFICATION THROUGH WAVELET-COMPRESSED SCATTERED ULTRAWIDE-BAND ELECTRIC FIELD DATA AND ROC ANALYSIS

S. Makal, A. Kizilay, and L. Durak

Yildiz Technical University
Electrical-Electronics Faculty
Electronics and Communications Engineering Department
Istanbul, Turkey

Abstract—This paper’s aim is to classify cylindrical targets from their ultrawide-band radar returns. To calculate the radar returns, image technique formulation is used to obtain the Electric Field Integral Equations (EFIEs). Then, the EFIEs are solved numerically by Method of Moment (MoM). Because of wide frequency range of the ultrawide-band radar signal, the database to be used for target classification becomes very large. To deal with this problem and to provide robustness, wavelet transform is utilized. Application of wavelet transform significantly reduces the size of the database. The coefficients obtained by wavelet transform are used as the inputs of the artificial neural networks (ANNs). Then, the actual performances of the networks are investigated by Receiver Operating Characteristic (ROC) analysis.

1. INTRODUCTION

Target identification from the radar scattering signatures is a complicated task; therefore, alternative approaches have been proposed, such as statistical models, fuzzy systems and artificial neural network (ANN) [1, 10]. Although ANNs are computationally intensive, they have become popular since late 80’s. The data reduction of the ANN inputs makes the network simpler, decreases the training time and the results usually become more robust. Various methods are applied to reduce the size of the ANN inputs. Wavelet packet decomposition for feature selection is proposed in [11] to obtain the coefficients to be used as ANN inputs for classifying underwater mines

and mine-like targets from the acoustic backscattered signals. A new approach of a wavelet-based radial basis function neural network is used to estimate the locations and radii of conducting cylindrical scatterers in [12].

This paper focuses the problem of cylindrical target classification. A cylindrical target with a radius of r_t is located at a distance h_t from the perfectly conducting (PEC) flat surface. The incident field E_i is a plane electromagnetic wave illuminating the target with the incidence angle of ϕ_i as shown in Fig. 1. Here, the location of the cylinder is denoted by the coordinates (x_0, y_0) on the xy -plane.

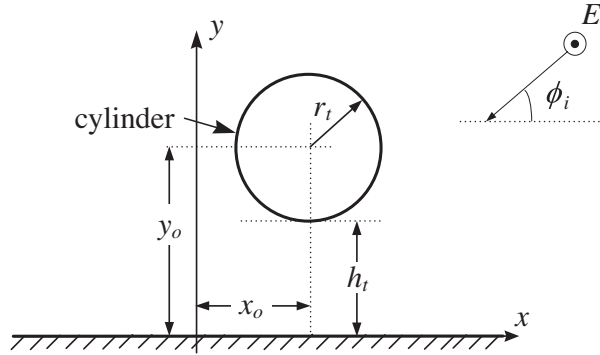


Figure 1. The geometry of the problem for a cylinder above an infinite flat surface.

For this scattering problem, the PEC flat surface is chosen to be infinitely long to avoid direct and indirect reflections from edges. The method of images can be employed to replace the infinite flat surface with images of the incident field and the cylinder. MoM [13] is used to solve the EFIEs to obtain the induced current on the target. After these derivations, the scattered electric field is expressed as,

$$E_z^s(\vec{r}) = -\eta_0 \sqrt{\frac{-jk_0}{8\pi}} \frac{e^{jk_0 r}}{\sqrt{r}} \left[\sum_{n=1}^{N_T} a_n^T \int_{L_n} e^{jk_0(x' \cos \phi_s + y' \sin \phi_s)} dl' \right] \quad (1)$$

where ϕ_s is the scattering angle, k_0 is the free-space wave number, \vec{r} is the position vector, η_0 is the intrinsic impedance of free space, L_n is the surface segment where the current is defined, and N_T is the number of the points on the cylinder [14].

In our previous work in [15], narrow band signals have been employed for target identification. The real and imaginary parts of the field of each frequency band formed some inputs of the ANNs.

Contrary to the previous work, here the whole signal is applied as the inputs of the ANNs after compressing by wavelet transform.

Fig. 2 presents the block diagram of the inputs and outputs of the method of images and EFIE-MoM solution. Frequency domain results are obtained by sweeping the frequency from 1 GHz to 30 GHz range with a step size of 0.04 GHz, resulting in 726 frequency data points.

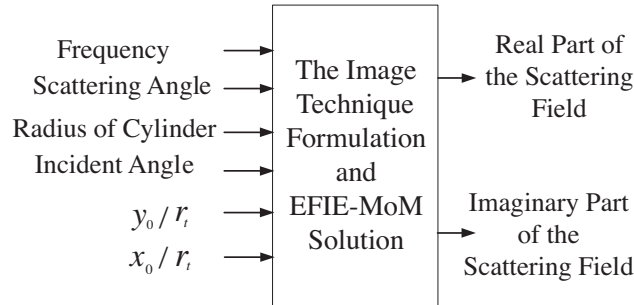


Figure 2. The block diagram of the inputs and outputs of the method of images and EFIE-MoM solution.

2. WAVELET TRANSFORM BASED SCATTERED ELECTRIC FIELD DATA COMPRESSION

The wavelet transform analyzes a signal by decomposing it into approximation and detail parts by filter banks [16]. Fig. 3 demonstrates the scheme of an analysis bank. At the first level, it employs a low-pass filter with transfer function H_0 , giving approximation coefficients and a high-pass filter with transfer function H_1 giving detail coefficients. At each level, filtering process is followed by a decimation by 2 that restricts the output data size.

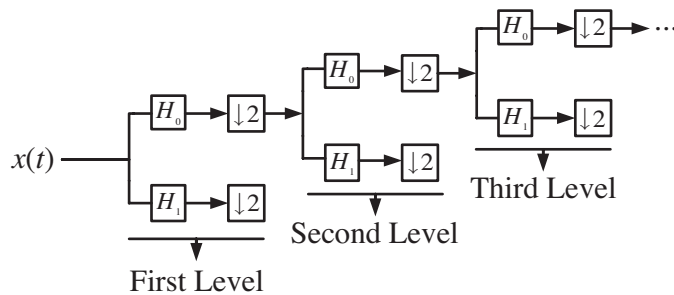


Figure 3. The filter bank.

Then, the low and high-pass filters are applied subsequently and output of the low-pass filter is down sampled by a factor of 2 to resolve high and low-frequency components [17]. In this work, low-frequency components of the signal are analyzed. Three-level Daubechies (db10) wavelet transform is used. Fig. 4 presents the low-frequency components of the signal at each level. Apparently, as the level order increases, more and more detail information is eliminated.

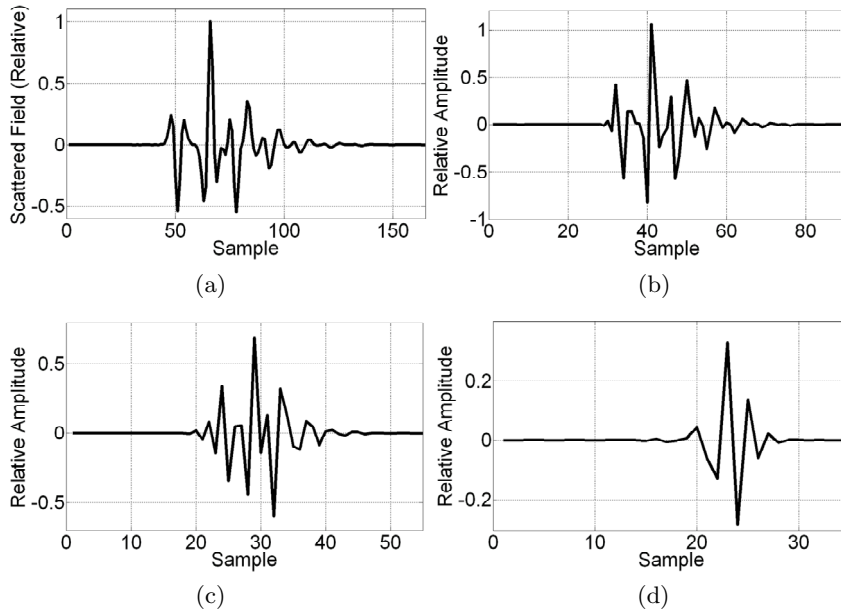


Figure 4. (a) Original signal, (b) first level, (c) second level, and (d) third level decomposition.

In the simulations, the variation of the scattered field is observed and the most energetic part of the data is selected as the inputs of the ANN. At the third level, this part corresponds to the coefficients between 18-27th samples.

3. ANN APPLICATION OF THE COMPRESSED DATA

The total number of scattering field vectors belonging to the two cylindrical targets is 34, where each data pair corresponds to a different angle. One half of the database is used to train the network, the other half is used to test the network.

Cross validation is applied to find the generalization ability of

ANN classification. In the hold-out method, which is the simple kind of cross validation, the data set is separated into two sets, called the training set and the testing set. In the k -fold cross-validation, the original sample is partitioned into k subset. A single subset is retained as the testing data and the remaining $k - 1$ subsets are used as training data. Then, the k results of testing and training can be averaged to produce a single estimation. Namely, in the k -fold cross validation, the data set is divided into k subsets, and the holdout method is repeated k times [18]. In this work, k is chosen as 2.

As seen in Fig. 5, wavelet coefficients are the inputs of the neural networks and the total number of inputs is 10. Radial basis function (RBF) neural network, general regression neural network (GRNN) and multilayer perceptron (MLP) are used to classify the targets.

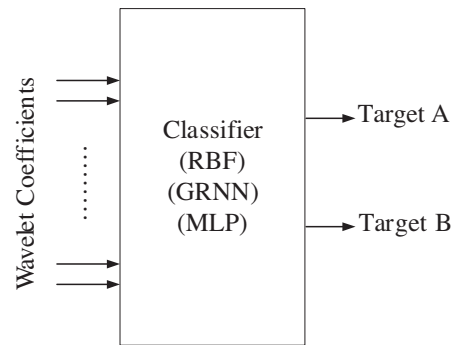


Figure 5. The block diagram of the classifier.

3.1. Radial Basis Function Network

RBF network is a two layer feed-forward neural network using radial basis functions as shown in Fig. 6. Such a network is characterized by a set of inputs and a set of outputs. In between the inputs and outputs there is a layer of processing units called hidden units. Each of them implements a radial basis function. The way in which the network is used for data modeling is different when approximating time-series and in pattern classification [19, 21].

Given the inputs x_j , the total input to the i th hidden neuron γ_i is given by

$$\gamma_i = \sqrt{\sum_{j=1}^n \left(\frac{x_j - c_{ij}}{\lambda_{ij}} \right)^2} \quad (2)$$

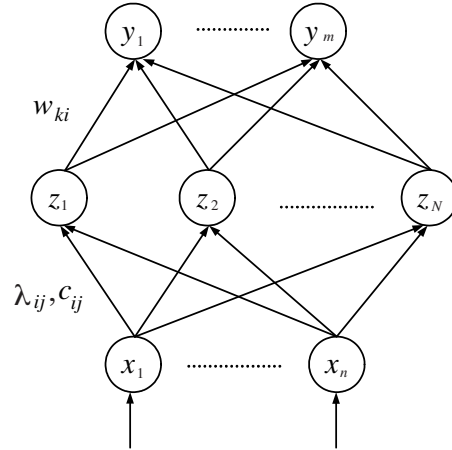


Figure 6. RBF network structure.

for $i = 1, 2, \dots, N$, where, N is the number of hidden neurons. The output value of the i th hidden neuron is $z_{ij} = \sigma(\gamma_i)$, where $\sigma(\gamma)$ is a radial basis function. The outputs of the RBF network are computed from hidden neurons as

$$y_k = \sum_{i=0}^N w_{ki} z_{ki} \quad (3)$$

where, w_{ki} is the weight of the link between the i th neuron of the hidden layer and the k th neuron of the output layer. Training parameters of the RBF network consists of w_{ki} , c_{ij} , and λ_{ij} for $k = 1, 2, \dots, m$, $i = 1, 2, \dots, N$, and $j = 1, 2, \dots, n$ [22, 23].

3.2. General Regression Neural Network

GRNN is a specific model of RBF network used for function approximation problems. These networks have a high success rate on approximation of continuous functions with an appropriate number of hidden neurons. Repeated training is not required as in MLP. As the dimensions of training data set are increased, the error rate approximates to zero. Kernel approach which is a statistical method is used in GRNN. According to this approach, a dependant y variable's regression to an independent x variable approximates to the most probable value of y for a given x input and training set. GRNN structure is seen in Fig. 7 and here, w_{mn} is assigned as the weight matrix of target value stated from the training set [24].

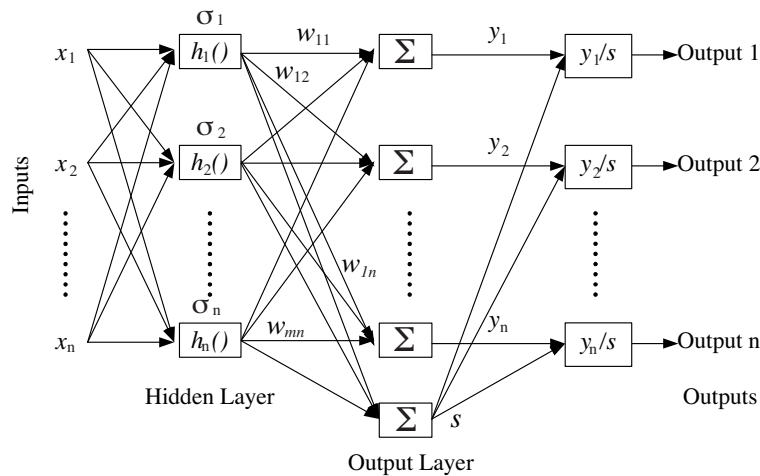


Figure 7. GRNN network structure.

3.3. Multilayer Perceptron

Multilayer perceptrons (MLPs) are feed-forward neural networks trained with the standard back propagation algorithm. They are supervised networks, therefore they require a desired response to be trained. They are widely used for pattern classification because they learn how to transform input data into a desired response.

MLP network has a highly connected topology since every input is connected to all nodes in the first hidden layer; every unit in the hidden layers is connected to all nodes in the next layer. With one or two hidden layers, they can approximate virtually any input-output map. The basic MLP building unit is a simple model of artificial neuron. This unit computes the weighted sum of the inputs plus the threshold weight and passes this sum through the activation function. The MLP structure is shown in Fig. 8, here, x_1, x_2, \dots, x_D are the inputs and y_1, y_2, \dots, y_N are the outputs of ANN. The output units in one layer form the inputs to the next layer. The weights of the network are usually computed by training the network using the back propagation algorithm [25, 26].

In these simulations, Levenberg-Marquardt algorithm (LMA) that provides a numerical solution to the mathematical problem of a function is used. It is the most popular curve-fitting algorithm and it is used almost in any software that supplies a generic curve-fitting tool [27].

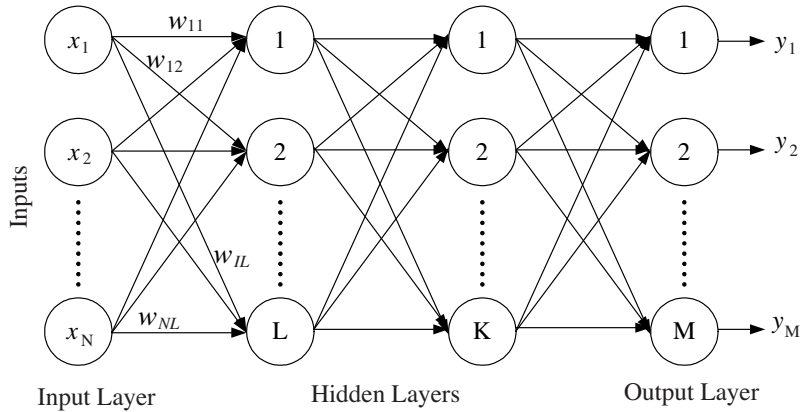


Figure 8. MLP network structure.

4. RESULTS OF THE ARTIFICIAL NEURAL NETWORKS

All networks have ten inputs and one output that determines in which cylinder scattering takes place. The spread value is chosen 0.9 for RBF neural network and 0.1 for GRNN. MLP network has one hidden layer of ten hidden units. Logarithmic sigmoid and saturating linear functions are used in hidden and output layers; respectively. MLP network is trained 50 epochs. The learning rate and the momentum constant are chosen 0.9. The average classification accuracies of MLP, RBF and GRNN are listed in Table 1. MLP has apparently the highest success rate.

Table 1. Success rates of the networks for testing and training data sets.

	Success Rate (%)	
	Testing	Training
RBF	79.41	97
GRNN	73.5	100
MLP	91.2	100

5. ROC ANALYSIS

As testing and training rate are not enough to analyze the sensitivities of the networks, ROC analysis is applied to find out the real performances of the networks used to classify the data set.

ROC analysis is related in a direct and natural way to cost/benefit analysis of diagnostic decision making. It is originated from signal detection theory, as a model of how well a receiver is able to detect a signal in the presence of noise. There are four possible outcomes from a binary classifier. If the outcome from a prediction is p and the actual value is also p , then it is called a true positive (TP); however if the actual value is n , then it is said a false positive (FP). Conversely, a true negative (TN) has occurred when both the prediction outcome and the actual value are n , and false negative (FN) is when the prediction outcome is n while the actual value is p [28]. In this work, p and n are defined as first target and second target respectively as shown in Table 2.

Table 2. ROC table.

		Actual Value	
		Target A	Target B
Predictions	Target A	TP	FP
	Target B	FN	TN

The limitations of diagnostic “accuracy” as a measure of decision performance require the introduction of concepts as the “sensitivity” and “specificity” of a diagnostic test. The equations of these measures can be expressed by (4) and (5) [29]:

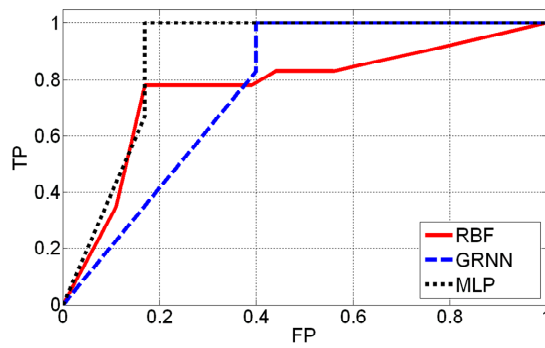
$$\text{Sensitivity} = \frac{\text{TP}}{\text{TP}+\text{FN}} \quad (4)$$

$$\text{Specificity} = \frac{\text{TN}}{\text{TN}+\text{FP}} \quad (5)$$

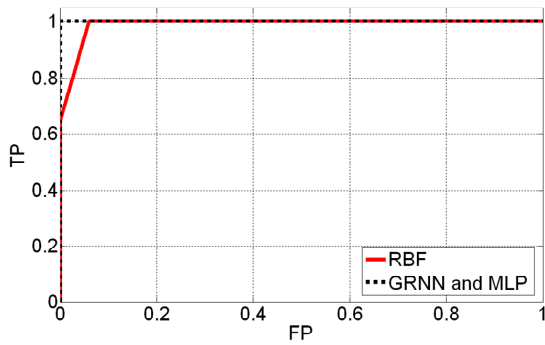
The sensitivity and specificity values of MLP, RBF and GRNN are demonstrated in Table 3. MLP has the highest values for both testing and training. ROC curves of testing and training are shown in Fig. 9. They demonstrate the relation between sensitivity and specificity. The area under the curve is a measure of testing and training accuracies. The closer to the left-hand border and then the top border of the ROC space the curve follows, the more successful the network is. In this work, MLP network has a better ROC curve than the other networks.

Table 3. Sensitivities and specificities values of the networks.

		Sensitivity	Specificity
RBF	Testing	0.78	0.83
	Training	1	0.95
GRNN	Testing	0.89	0.6
	Training	1	0.1
MLP	Testing	1	0.83
	Training	1	1



(a)



(b)

Figure 9. ROC curves of the networks for (a) testing and (b) training.

6. CONCLUSION

In this target classification analyses, the scattered electric field data at different angles from two cylindrical targets are compressed by wavelet transform. Therefore, the compressed inputs of the neural networks are determined and a dataset is formed. RBF, GRNN and MLP are investigated in this work. According to the testing and training rates, the best classifier is the MLP. To support this result, sensitivity and specificity values and the ROC curves are obtained and it is observed that MLP is better than the other networks. Consequently, classification of more targets is planned as a next step to this work by applying MLPs.

REFERENCES

1. Yang, Y., "MIMO radar waveform design based on mutual information and minimum mean-square error estimation," *IEEE Transactions on Aerospace and Electronic Systems*, Vol. 43, No. 1, 330–343, 2007.
2. Park, S. E., "Unsupervised classification of scattering mechanisms in polarimetric SAR data using fuzzy logic in entropy and alpha plane," *IEEE Transactions on Geoscience and Remote Sensing*, Vol. 45, No. 8, 2652–2664, 2007.
3. Turhan, G., "Real time electromagnetic target classification using a novel feature extraction technique with PCA-based fusion," *IEEE Transaction on Antennas and Propagation*, Vol. 53, No. 2, 766–776, 2005.
4. Chen, X., D. Liang, and K. Huang, "Microwave imaging 3-d buried objects using parallel genetic algorithm combined with FDTD technique," *J. of Electromagn. Waves and Appl.*, Vol. 20, No. 13, 1761–1774, 2006.
5. Xue, W. and X.-W. Sun, "Target detection of vehicle volume detecting radar based on Wigner-Hough transform," *Journal of Electromagnetic Waves and Applications*, Vol. 21, No. 11, 1513–1523, 2007.
6. Li, Y.-L., J.-Y. Huang, and M.-J. Wang, "Investigation of electromagnetic interaction between a spherical target and a conducting plane," *Journal of Electromagnetic Waves and Applications*, Vol. 21, No. 12, 1703–1715, 2007.
7. Alivizatos, E. G., M. N. Petsios, and N. K. Uzunoglu, "Towards a range-doppler UHF multistatic radar for the detection of

- noncooperative targets with low RCS,” *Journal of Electromagnetic Waves and Applications*, Vol. 19, No. 15, 2015–2031, 2005.
8. Lee, K.-C. and J.-S. Ou, “Radar target recognition by using linear discriminant algorithm on angular-diversity RCS,” *Journal of Electromagnetic Waves and Applications*, Vol. 21, No. 14, 2033–2048, 2007.
 9. Zainud-Deen, S. H., M. E. Badr, E. El-Deen, K. H. Awadalla, and H. A. Sharshar, “Microstrip antenna with corrugated ground plane surface as a sensor for landmines detection,” *Progress In Electromagnetics Research B*, Vol. 2, 259–278, 2008.
 10. Ozdemir, C., S. Demirci, and E. Yigit, “Practical algorithms to focus B-scan GPR images: theory and application to real data,” *Progress In Electromagnetics Research B*, Vol. 6, 109–122, 2008.
 11. Azimi-Sadjadi, M. R., D. Yao, Q. Huang, and G. J. Dobeck, “Underwater target classification using wavelet packets and neural networks,” *IEEE Trans. on Neural Networks*, Vol. 11, No. 3, 784–794, 2000.
 12. Ak, U., T. Gnel, and I. Erer, “A wavelet-based radial-basis function neural network approach to the conducting cylinders,” *Microwave and Optical Technology Letters*, Vol. 41, No. 6, 506–511, 2004.
 13. Hassani, H. R. and M. Jahanbakht “Method of moment analysis of finite phased array of aperture coupled circular microstrip patch antennas,” *Progress In Electromagnetics Research B*, Vol. 4, 197–210, 2008.
 14. Kizilay, A. and S. Makal, “A neural network solution for identification and classification of cylindrical targets above perfectly conducting flat surfaces,” *Journal of Electromagnetic Waves and Applications*, Vol. 21, No. 14, 2147–2156, 2007.
 15. Kizilay, A., “A perturbation method for transient multipath analysis of electromagnetic scattering from targets above periodic surfaces,” Ph.D. dissertation, Michigan State University, 2000.
 16. Strang, G. and T. Nyugen, *Wavelets and Filterbanks*, Wellesley-Cambridge Press, Massachusetts, 1997.
 17. Arivazhagan, S., W. S. L. Jebarani, and G. Kumaran, “Performance comparison of discrete wavelet transform and dual tree discrete wavelet transform for automatic airborne target detection,” *International Conference on Computational Intelligence and Multimedia Applications*, 495–500, 2007.
 18. Zhang, R., G. McAllister, B. Scotney, S. McClean, and G. Houston, “Combining wavelet analysis and Bayesian networks

- for the classification of auditory brainstem response,” *IEEE Transactions on Information Technology in Biomedicine*, Vol. 10, No. 3, 458–467, 2006.
19. Bors, A. G. and M. Gabbouj, “Neural networks and radial basis function neural network for pattern classification,” *Digital Signal Processing: A Review Journal*, Vol. 4, No. 3, 173–188, 1994.
 20. Zainud-Deen, S. H., H. A. Malhat, K. H. Awadalla, and E. S. El-Hadad, “Direction of arrival and state of polarization estimation using radial basis function neural network (RBFNN),” *Progress In Electromagnetics Research B*, Vol. 2, 137–150, 2008.
 21. Mohamed, M. D. A., E. A. Soliman, and M. A. El-Gamal, “Optimization and characterization of electromagnetically coupled patch antennas using RBF neural networks,” *Journal of Electromagnetic Waves and Applications*, Vol. 20, No. 8, 1101–1114, 2006.
 22. Park, J. and W. I. Sandberg, “Universal approximation using radial basis function networks,” *Neural Computation*, Vol. 3, No. 2, 246–257, 1991.
 23. Mohamed, M. D. A., E. A. Soliman, and M. A. El-Gamal, “Optimization and characterization of electromagnetically coupled patch antennas using RBF neural networks,” *Journal of Electromagnetic Wave and Applications*, Vol. 20, No. 8, 1101–1114, 2006.
 24. Rutkowski, L., “Generalized regression neural networks in time-varying environment,” *IEEE Transactions on Neural Networks*, Vol. 15, No. 3, 576–596, 2004.
 25. Haykin, S., *Neural Networks: A Comprehensive Foundation*, Macmillan College Publishing, New York, 1994.
 26. Guney, K., C. Yildiz, S. Kaya, and M. Turkmen, “Artificial neural networks for calculating the characteristic impedance of air-suspended trapezoidal and rectangular-shaped microshield lines,” *Journal of Electromagnetic Waves and Applications*, Vol. 20, No. 9, 1161–1174, 2006.
 27. Schalkoff, R. J., *Artificial Neural Networks*, McGraw-Hill Inc., Singapore, 1997.
 28. Sboner, A., “Multiple classifier system for early melanoma diagnosis,” *AI in Medicine*, Vol. 27, No. 1, 29–44, 2003.
 29. Wang, S., C. I. Chang, S. C. Yang, G. C. Hsu, H. H. Hsu, P. C. Chung, S. M. Gua, and S. K. Lee, “3D ROC analysis for medical imaging diagnosis,” *IEEE International Conference of the Engineering in Medicine and Biology*, 7545–7548, 2005.